

# Essential role of Skp2-mediated p27 degradation in growth and adaptive expansion of pancreatic $\beta$ cells

Lingwen Zhong, Senta Georgia, Shuen-ing Tschen, Keiko Nakayama, Keiichi Nakayama, Anil Bhushan

*J Clin Invest.* 2007;117(10):2869-2876. <https://doi.org/10.1172/JCI32198>.

Research Article Metabolism

Diabetes results from an inadequate mass of functional  $\beta$  cells, due to either  $\beta$  cell loss caused by immune assault or the lack of compensation to overcome insulin resistance. Elucidating the mechanisms that regulate  $\beta$  cell mass has important ramifications for fostering  $\beta$  cell regeneration and the treatment of diabetes. We report here that Skp2, a substrate recognition component of Skp1–Cul1–F-box (SCF) ubiquitin ligase, played an essential and specific role in regulating the cellular abundance of p27 and was a critical determinant of  $\beta$  cell proliferation. In *Skp2*<sup>-/-</sup> mice, accumulation of p27 resulted in enlarged polyploid  $\beta$  cells as a result of endoreduplication replacing proliferation. Despite  $\beta$  cell hypertrophy, *Skp2*<sup>-/-</sup> mice exhibited diminished  $\beta$  cell mass, hypoinsulinemia, and glucose intolerance. Increased insulin resistance resulting from diet-induced obesity caused *Skp2*<sup>-/-</sup> mice to become overtly diabetic, because  $\beta$  cell growth in the absence of cell division was insufficient to compensate for increased metabolic demand. These results indicate that the Skp2-mediated degradation pathway regulating the cellular degradation of p27 is essential for establishing  $\beta$  cell mass and to respond to increased metabolic demand associated with insulin resistance.

**Find the latest version:**

<https://jci.me/32198/pdf>





# Essential role of Skp2-mediated p27 degradation in growth and adaptive expansion of pancreatic $\beta$ cells

Lingwen Zhong,<sup>1</sup> Senta Georgia,<sup>1,2</sup> Shuen-ing Tschen,<sup>1</sup> Keiko Nakayama,<sup>3</sup> Keiichi Nakayama,<sup>3</sup> and Anil Bhushan<sup>1,2</sup>

<sup>1</sup>Larry Hillblom Islet Research Center and <sup>2</sup>Molecular Biology Institute, David Geffen School of Medicine, UCLA, Los Angeles, California, USA.

<sup>3</sup>CREST, Japan Science and Technology Corporation, Kawaguchi, Saitama, Japan.

**Diabetes results from an inadequate mass of functional  $\beta$  cells, due to either  $\beta$  cell loss caused by immune assault or the lack of compensation to overcome insulin resistance. Elucidating the mechanisms that regulate  $\beta$  cell mass has important ramifications for fostering  $\beta$  cell regeneration and the treatment of diabetes. We report here that Skp2, a substrate recognition component of Skp1-Cul1-F-box (SCF) ubiquitin ligase, played an essential and specific role in regulating the cellular abundance of p27 and was a critical determinant of  $\beta$  cell proliferation. In  $Skp2^{-/-}$  mice, accumulation of p27 resulted in enlarged polyploid  $\beta$  cells as a result of endoreduplication replacing proliferation. Despite  $\beta$  cell hypertrophy,  $Skp2^{-/-}$  mice exhibited diminished  $\beta$  cell mass, hypoinsulinemia, and glucose intolerance. Increased insulin resistance resulting from diet-induced obesity caused  $Skp2^{-/-}$  mice to become overtly diabetic, because  $\beta$  cell growth in the absence of cell division was insufficient to compensate for increased metabolic demand. These results indicate that the Skp2-mediated degradation pathway regulating the cellular degradation of p27 is essential for establishing  $\beta$  cell mass and to respond to increased metabolic demand associated with insulin resistance.**

## Introduction

Increasing evidence suggests that variations in insulin demand as a result of physiological and pathological states such as aging, pregnancy, and obesity can lead to adaptive changes in the  $\beta$  cells that include hyperplasia, hypertrophy, and increased insulin synthesis and secretion (1–4). How  $\beta$  cells respond to changing metabolic demands to regulate  $\beta$  cell mass in order to maintain glucose homeostasis is unclear. The inability of the endocrine pancreas to adapt to the changing insulin demand can result in hyperglycemia and development of diabetes mellitus (5–7). Thus, deciphering the mechanisms that regulate the plasticity of  $\beta$  cell mass can be important in developing effective strategies to treat diabetes. Several recent studies have highlighted the role of cell cycle regulators in establishing  $\beta$  cell mass (reviewed in refs. 8–11). These studies indicate that the balance between cyclin D2-Cdk4 complexes (12) that form in response to mitotic signals and cyclin kinase inhibitors that block the activity of cyclin E-Cdk2 complexes regulates  $\beta$  cell proliferation. We have recently shown that quiescent  $\beta$  cells accumulate p27 and that disabling p27 in these cells allows them to divide (13). Thus, the cellular abundance of p27 is a critical determinant of whether a  $\beta$  cell divides or remains quiescent. Furthermore, deletion of p27 ameliorated hyperglycemia in animal models of type 2 diabetes, suggesting that p27 represents a potential new target for treatment of diabetes (14).

The cellular abundance of p27 is normally subject to precise regulation by the ubiquitin-mediated proteolytic pathway (15). Covalent attachment of ubiquitin to p27 by ubiquitin ligases signals its destruction by the 26S proteosome. Specificity in proteolysis by the

ubiquitin-proteosome system is governed largely by the action of specific subunits of the ubiquitin ligase complexes that recognize and bind to p27. Two families of ubiquitin ligases, Skp1-Cul1-F-box (SCF) and APC, regulate p27 destruction and play crucial roles in cell duplication. During the S phase, degradation of p27 is promoted by its phosphorylation on Thr<sup>187</sup> by the cyclin E-Cdk2 complex (16–18). Skp2, an F-box protein, functions as a receptor component of an SCF ubiquitin ligase complex and binds to p27 only when Thr<sup>187</sup> is phosphorylated, resulting in ubiquitination and subsequent degradation (19–22).

Here we analyzed the role of Skp2-mediated p27 degradation in regulating  $\beta$  cell mass during normal growth and in adaptive changes caused by increased insulin resistance. We show that Skp2 was required for the degradation of p27 in  $\beta$  cells. Accumulation of p27 in  $Skp2^{-/-}$  mice prevented proliferation and led to endoreduplication (when cells undergo DNA synthesis without mitosis) of  $\beta$  cells. The inability of  $\beta$  cells to proliferate in the absence of Skp2 resulted in decreased  $\beta$  cell mass, hypoinsulinemia, and a corresponding decrease in the ability to dispose glucose from blood. Moreover, increased insulin resistance in the absence of p27 degradation hampered compensatory increases in the  $\beta$  cell mass, thus leading to overt diabetes. These results suggest that Skp2-mediated p27 degradation within  $\beta$  cells could play a role in translating metabolic demands into regulation of  $\beta$  cell mass.

## Results

To address whether Skp2 regulates the accumulation of p27 in  $\beta$  cells, we analyzed the expression of p27 in islets derived from mice in which Skp2 had been inactivated by homologous recombination in ES cells (23). Pancreatic sections from 3-week-old wild-type,  $Skp2^{+/+}$ , and  $Skp2^{-/-}$  mice were analyzed for the expression of p27 and insulin. A number of  $\beta$  cells in the wild-type and  $Skp2^{+/+}$  pancreata did not show any accumulation of p27 in the nucleus

**Nonstandard abbreviations used:** HFD, high-fat diet; ND, normal diet; pH3, phospho-histone H3; SCF, Skp1-Cul1-F-box.

**Conflict of interest:** The authors have declared that no conflict of interest exists.

**Citation for this article:** *J. Clin. Invest.* 117:2869–2876 (2007). doi:10.1172/JCI32198.

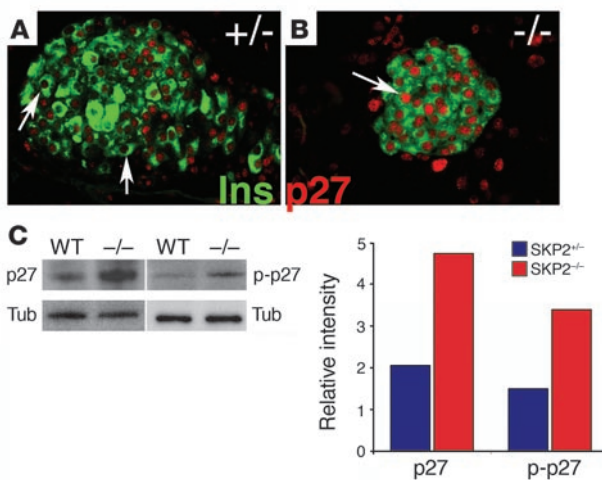


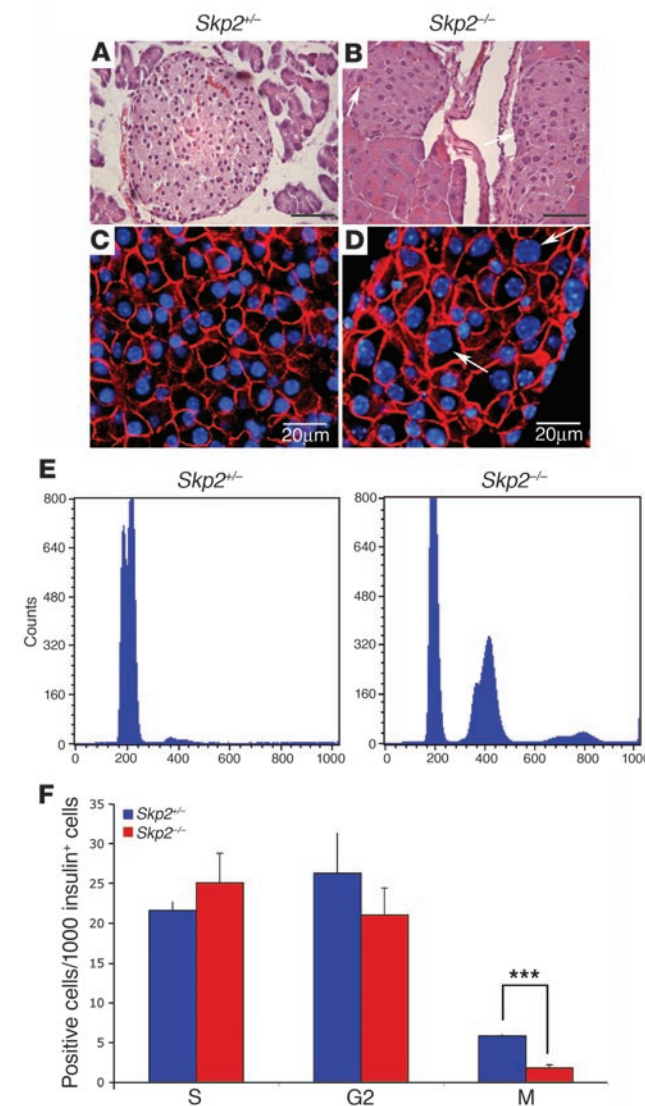
(Figure 1A). By contrast, all  $\beta$  cells in  $Skp2^{-/-}$  pancreata showed high levels of p27 protein accumulation in the nucleus (Figure 1B). Because further morphological and metabolic analyses showed no discernable difference between wild-type and  $Skp2^{+/+}$  mice, we used  $Skp2^{+/+}$  littermates as controls in analyzing  $Skp2^{-/-}$  mice. To confirm the increased accumulation of p27 protein, islets isolated from  $Skp2^{-/-}$  and  $Skp2^{+/+}$  littermate pancreata was subjected to immunoblot analysis. The increase in accumulation of p27 protein was apparent in  $Skp2^{-/-}$  islets compared with islets from  $Skp2^{+/+}$  littermates (Figure 1C). Because Skp2 ubiquitinates and degrades phospho-p27, we also used a phospho-Thr<sup>187</sup> site-specific antibody for p27 to show that the phosphorylated form of p27 accumulated in  $Skp2^{-/-}$  islet (17).

To assess whether cellular accumulation of p27 affected islet formation, we examined the morphology of islets in pancreata from mice 10 weeks after birth. Hematoxylin and eosin staining revealed a striking reduction in the size of islets in the pancreata from  $Skp2^{-/-}$  mice compared with that of their littermates (Figure 2, A and B). Further examination revealed that the size of the nuclei in  $Skp2^{-/-}$  islets was markedly larger than that of  $Skp2^{+/+}$  littermates. To verify the increase in nuclear and cell size, pancreatic sections from 10-week-old mice were stained with  $\beta$ -catenin and DAPI to mark the cell membranes and nuclei, respectively. The nuclei in  $Skp2^{-/-}$  islets were discernibly larger than those in islets from  $Skp2^{+/+}$  littermates (Figure 2, C and D). Flow cytometry demonstrated that a significant portion of the cells from  $Skp2^{-/-}$  islets exhibited polyploidy (4C or higher), whereas most of the cells from

**Figure 1**

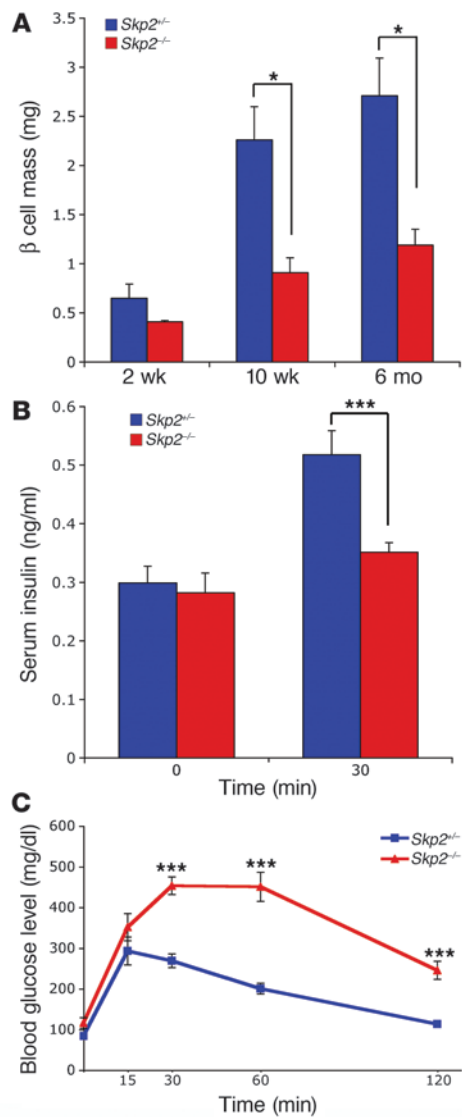
Deletion of Skp2 resulted in the accumulation of p27 protein in pancreatic islet cells. (A and B) Pancreatic sections from 3-week-old  $Skp2^{+/+}$  (A) and  $Skp2^{-/-}$  (B) mice were immunostained with anti-mouse insulin (green) and anti-mouse p27 (red) antibodies. Original magnification,  $\times 20$ . Arrows in A show  $\beta$  cells that do not express p27 in wild-type islets. Arrows in B show high levels of accumulated p27 in  $\beta$  cells in  $Skp2^{-/-}$  islets. (C) Immunoblot analysis of p27 and phospho-p27 (p-p27) expression in the islet cells isolated from  $Skp2^{+/+}$  and  $Skp2^{-/-}$  pancreata. Graph demonstrates densitometric analysis of immunoblot of p27 and phospho-p27 normalized to tubulin. For all panels, data are representative of 3 experiments.

$Skp2^{+/+}$  littermate islets had a DNA content of 2C (Figure 2E). To analyze the reason for polyploid islet cells in the  $Skp2^{-/-}$  mice, we compared the cell cycle characteristics of  $\beta$  cells from  $Skp2^{-/-}$  and  $Skp2^{+/+}$  littermates. The number of S- and G2-phase  $\beta$  cells, as assessed by BrdU pulse labeling and phospho-histone H3 (pHH3) staining, did not change in  $Skp2^{-/-}$  mice compared with  $Skp2^{+/+}$  littermates. By contrast, the M-phase  $\beta$  cells were greatly reduced in the  $Skp2^{-/-}$  mice compared with  $Skp2^{+/+}$  littermates (Figure 2F).



**Figure 2**

Endoreduplication resulted in polyploidy  $\beta$  cells in  $Skp2^{-/-}$  mice. (A–D) Morphological analysis of pancreatic islets from 10-week-old  $Skp2^{+/+}$  (A and C) and  $Skp2^{-/-}$  (B and D) mice. Pancreatic sections were stained with hematoxylin and eosin (A and B) or with  $\beta$ -catenin (red) and DAPI (blue) (C and D). Arrows in B indicate enlarged nuclei. Arrows in D show an enlarged cell in the  $Skp2^{-/-}$  islet. Scale bars: 20  $\mu$ m. (E) Flow cytometric analysis of DNA content of islet cells isolated from  $Skp2^{+/+}$  and  $Skp2^{-/-}$  pancreata. (F) Cell cycle characteristics of  $\beta$  cells from  $Skp2^{+/+}$  and  $Skp2^{-/-}$  mice as measured by BrdU pulse labeling and pHH3 staining. BrdU<sup>+</sup>insulin<sup>+</sup> cells are counted as  $\beta$  cells at S phase. pHH3<sup>+</sup> (with punctuated pattern) insulin<sup>+</sup> cells are counted as  $\beta$  cells at G2 phase. pHH3<sup>+</sup> (with strong nuclear expression) insulin<sup>+</sup> cells are counted as  $\beta$  cells at M phase. At least 2,000  $\beta$  cells were counted at each cell cycle phase. Data are mean  $\pm$  SEM. \*\*\*P < 0.005.


**Figure 3**

Decreased  $\beta$  cell mass, impaired glucose metabolism, and hypoinsulinemia in  $Skp2^{-/-}$  mice. (A) Analysis of  $\beta$  cell mass of  $Skp2^{+/−}$  and  $Skp2^{-/-}$  mice at 2 weeks, 10 weeks, and 6 months of age. Values are representative of 5 slides spanning the whole pancreas of each mouse and 3 mice per genotype at each age. (B) Serum insulin levels in  $Skp2^{+/−}$  and  $Skp2^{-/-}$  mice before and 30 minutes after glucose injection i.p. following overnight fast.  $n = 3$  per group. (C) Glucose tolerance test. Ten-week-old  $Skp2^{+/−}$  and  $Skp2^{-/-}$  mice were fasted overnight, and the blood glucose level was measured before and after glucose challenge. Differences were significant between groups at 30, 60, and 120 minutes ( $P < 0.001$  for all comparisons).  $n = 5$  ( $Skp2^{+/−}$ ); 8 ( $Skp2^{-/-}$ ). \* $P < 0.05$ ; \*\*\* $P < 0.005$ .

overnight fasting were similar in  $Skp2^{+/−}$  and  $Skp2^{-/-}$  mice. However, 30 minutes after glucose challenge, serum insulin levels almost doubled in  $Skp2^{+/−}$  mice but only increased slightly in  $Skp2^{-/-}$  mice (Figure 3B). The  $Skp2^{-/-}$  mice had fasting blood glucose levels that were slightly elevated compared with those of  $Skp2^{+/−}$  mice.  $Skp2^{-/-}$  mice also showed a decreased ability to clear glucose from the blood following i.p. glucose injection. The blood glucose of  $Skp2^{+/−}$  mice peaked at levels between 270 and 300 mg/dl 15 minutes after injection and reached baseline by the end of the 120-minute testing period (Figure 3C). In contrast,  $Skp2^{-/-}$  mice had elevated blood glucose levels (450–500 mg/dl) 30 minutes after injection. Moreover, the blood glucose levels failed to return to baseline levels during the testing period and remained in the range of 270–300 mg/dl at 120 minutes after injection. As described below, insulin tolerance test showed no detectable difference in the insulin sensitivity in  $Skp2^{-/-}$  and  $Skp2^{+/−}$  littermate mice, indicating that loss of  $Skp2$  by itself did not result in insulin resistance.

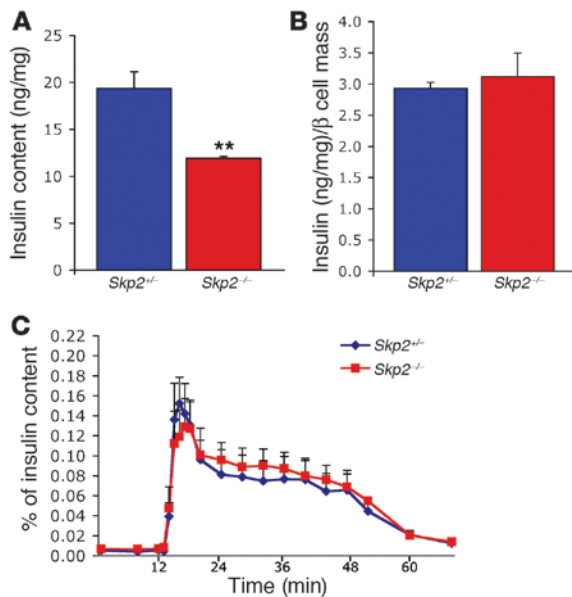
Because the loss of  $Skp2$  resulted in increased cell and nuclear size of  $\beta$  cells, we determined whether the insulin content and secretion characteristics of these  $\beta$  cells were altered. Consistent with the reduced  $\beta$  cell mass of  $Skp2^{-/-}$  mice, total insulin content was correspondingly decreased in these pancreata (Figure 4A). When normalized to  $\beta$  cells mass, however, no difference in insulin content was observed in the pancreata derived from  $Skp2^{-/-}$  and  $Skp2^{+/−}$  littermates (Figure 4B). This indicated that the amount of insulin produced in the  $\beta$  cells of  $Skp2^{-/-}$  pancreas was not likely to be changed by the absence of  $Skp2$ . We next investigated whether islets from  $Skp2^{-/-}$  and  $Skp2^{+/−}$  littermates display differences in their insulin secretion characteristics. Isolated islets from  $Skp2^{-/-}$  mice exposed to basal glucose (4 mM) secreted insulin at a relative steady state. Following the step increase in perfuse glucose concentration, there was a rapid increase in insulin secretion that peaked 10 minutes after increased glucose stimulation and then gradually returned to steady-state levels at 60 minutes. The insulin secretion characteristics in islets isolated from  $Skp2^{-/-}$  mice did not differ from those of  $Skp2^{+/−}$  littermates (Figure 4C). These results indicated that the polyploid  $\beta$  cells generated in the absence of  $Skp2$  did not change their functional characteristics with respect to glucose-stimulated insulin secretion.

To determine whether the accumulation of p27 is essential for generating the  $\beta$  cell polyploidy that led to reduced  $\beta$  cell mass and impaired glucose metabolism in  $Skp2^{-/-}$  mice, we generated double-mutant mice that lacked both  $Skp2$  and p27. Deletion of 1 allele of p27 in the  $Skp2^{-/-}$  background was not sufficient to restore the size of  $\beta$  cells, because a number of characteristic enlarged  $\beta$  cells were clearly evident in the islets of these mice, although more heteroge-

Taken together, these analyses indicated that accumulation of p27 as a result of absence of  $Skp2$  prevented proliferation and resulted in endoreduplication of  $\beta$  cells.

We next assessed whether the substitution of endoreduplication for proliferation in the  $Skp2^{-/-}$  mice affected the growth and function of  $\beta$  cells. We have previously shown that in the 2 months after birth, proliferation of  $\beta$  cells leads to a 4-fold increase in  $\beta$  cell mass as the endocrine pancreas adapts to the metabolic demands of growth (24). As expected, the  $Skp2^{+/−}$  mice showed a 4-fold increase in  $\beta$  cell mass between 2 and 10 weeks of age. By contrast, the  $Skp2^{-/-}$  mice did not show similar increases in  $\beta$  cell mass, and by 10 weeks of age displayed a 3-fold decrease in  $\beta$  cell mass compared with  $Skp2^{+/−}$  littermates (Figure 3A). The disparity in  $\beta$  cell mass between  $Skp2^{-/-}$  and  $Skp2^{+/−}$  littermate was evident into adulthood: 6-month-old  $Skp2^{-/-}$  mice also showed the same relative difference in  $\beta$  cell mass.

To test whether the reduced  $\beta$  cell mass of  $Skp2^{-/-}$  mice results in altered serum insulin levels and abnormal glucose homeostasis, we measured serum insulin levels and performed glucose tolerance tests in  $Skp2^{+/−}$  and  $Skp2^{-/-}$  mice. The serum insulin levels after



neity in beta cell size was observed compared with *Skp2<sup>−/−</sup>* islets (Figure 5A). By contrast, pancreatic sections from double-mutant mice did not display enlarged beta cells characteristic of *Skp2<sup>−/−</sup>* islets, and the size of the nuclei was similar to that of wild-type beta cells (Figure 5B). The lack of enlarged beta cells indicated that the absence of p27 completely restored beta cell proliferation. Analysis of beta cell mass (Figure 5C) showed that the beta cell mass of *p27<sup>+/−</sup>/Skp2<sup>−/−</sup>* mice, while increased compared with that of *Skp2<sup>−/−</sup>* mice, was significantly less than the beta cell mass of double mutants and similar to that of *p27<sup>−/−</sup>* mice (13). Metabolic analysis showed that *p27<sup>+/−</sup>/Skp2<sup>−/−</sup>* mice displayed decreased ability to clear glucose from blood following i.p. glucose injection and were glucose intolerant (Figure 5C). Thus the absence of 1 allele of *p27* in the *Skp2<sup>−/−</sup>* background was not sufficient to restore glucose homeostasis. By contrast, the double-mutant mice displayed an ability to clear glucose from the blood that could not be distinguished from that of wild-type mice. These results indicated that loss of *p27* was sufficient to restore beta cell morphology and glucose homeostasis in the *Skp2<sup>−/−</sup>* mice, suggesting that accumulation of *p27* was primarily responsible for the observed phenotypes of *Skp2<sup>−/−</sup>* mice.

To determine whether Skp2-mediated *p27* degradation is required for the compensatory beta cell

**Figure 4**

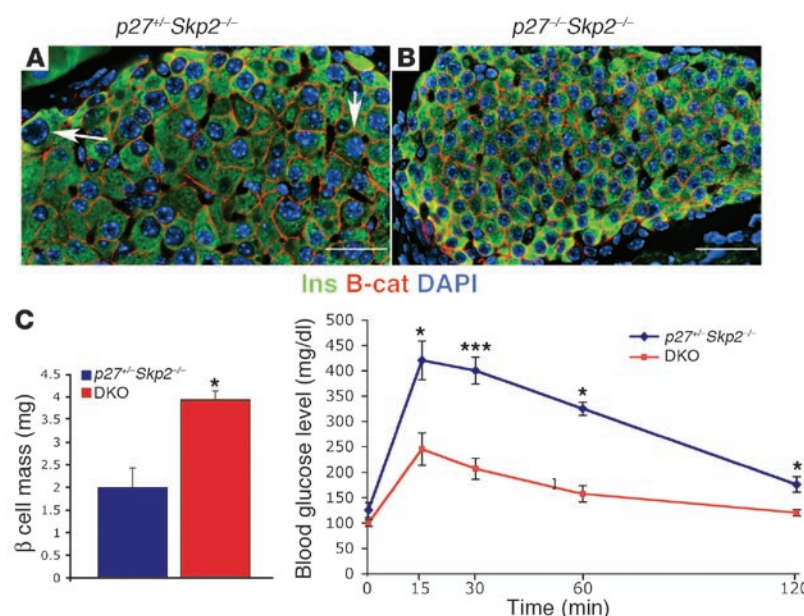
The absence of Skp2 does not affect insulin content and glucose-stimulated insulin secretion of beta cells. **(A and B)** Insulin content of *Skp2<sup>+/−</sup>* and *Skp2<sup>−/−</sup>* beta cells, which were normalized to pancreas weight (A) or to beta cell mass (B). *n* = 3 per group. **(C)** Glucose-induced insulin secretion of *Skp2<sup>+/−</sup>* and *Skp2<sup>−/−</sup>* beta cells was detected by in vitro islet perfusion assay. \*\**P* < 0.01.

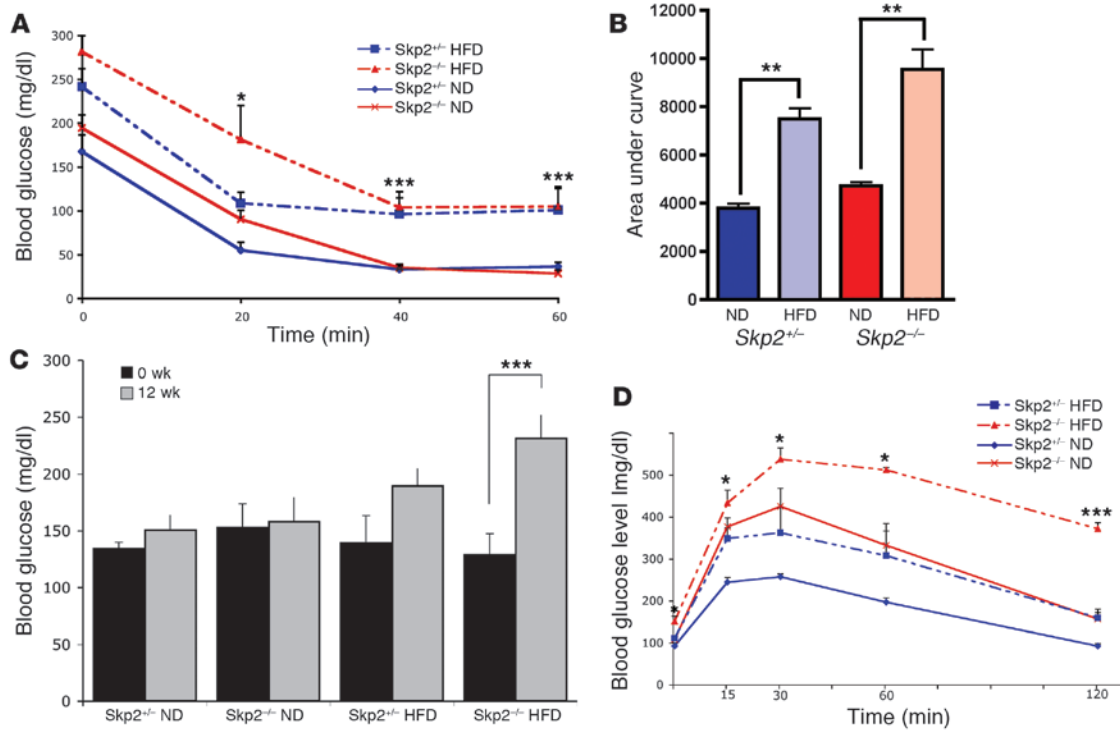
mass expansion in diet-induced insulin resistance, we subjected *Skp2<sup>−/−</sup>* and *Skp2<sup>+/−</sup>* littermates to a high-fat diet (HFD; 55% of total calories derived from fat, 4.8 kcal/g) for 12 weeks. Insulin tolerance test showed that all mice fed the HFD displayed decreased insulin sensitivity compared with mice fed normal diet (ND; Figure 6, A and B). However, fasting blood glucose measurements revealed that the *Skp2<sup>−/−</sup>* mice fed HFD were overtly diabetic, with fasting blood glucose consistently over 200 mg/dl. By contrast, the *Skp2<sup>+/−</sup>* littermates fed HFD did not display fasting blood glucose that was significantly different from that of *Skp2<sup>−/−</sup>* mice fed ND (Figure 6C). Glucose tolerance tests confirmed the worsened ability of *Skp2<sup>−/−</sup>* mice fed HFD to clear glucose from blood following i.p. glucose injection compared with *Skp2<sup>−/−</sup>* mice fed ND (Figure 6D). The glucose levels of *Skp2<sup>−/−</sup>* mice fed HFD reached 550 mg/dl by 30 minutes after injection and remained around 400 mg/dl by the end of the 120-minute testing period.

To assess whether the compensatory mechanisms that lead to changes in beta cell mass in the *Skp2<sup>−/−</sup>* mice fed HFD were affected, we carried out morphometric measurements of beta cell mass. The *Skp2<sup>−/−</sup>* mice fed HFD showed a 2-fold increase in beta cell mass compared with *Skp2<sup>+/−</sup>* mice fed ND. The *Skp2<sup>−/−</sup>* mice fed HFD by contrast showed modest increases in beta cell mass (Figure 7A). Immunostaining of pancreatic sections revealed that while the size of islets dramatically increased in *Skp2<sup>−/−</sup>* mice fed HFD, no change in the sizes of individual beta cells were observed relative to *Skp2<sup>+/−</sup>* mice fed ND (ND, 9.97 ± 0.11 μm; HFD, 10.02 ± 0.10 μm; Figure 7B). The *Skp2<sup>−/−</sup>* mice fed HFD by contrast displayed relatively smaller islets; however, the size of individual beta cells increased

**Figure 5**

Deletion of *p27* reverses the morphological and metabolic phenotype of *Skp2<sup>−/−</sup>* mice. **(A and B)** Morphological analysis of pancreatic islets from 10-week-old *p27<sup>+/−</sup>/Skp2<sup>−/−</sup>* (A) and *p27<sup>−/−</sup>/Skp2<sup>−/−</sup>* double-knockout (DKO; B) mice. Pancreatic sections were stained with beta-catenin (red) and DAPI (blue). White arrows point to the enlarged nuclear in *p27<sup>+/−</sup>/Skp2<sup>−/−</sup>* islets. Scale bars: 50 μm. **(C)** Increase in beta cell mass was greater in 10-week-old double-knockout mice than in *p27<sup>+/−</sup>/Skp2<sup>−/−</sup>* mice. *n* = 3 per group. **(D)** Impaired glucose tolerance was restored in 10-week-old double-knockout mice compared with that in *p27<sup>+/−</sup>/Skp2<sup>−/−</sup>* mice. *n* = 3 per group. \**P* < 0.05; \*\*\**P* < 0.005.




**Figure 6**

*Skp2*<sup>−/−</sup> mice failed to compensate for diet-induced insulin resistance. (A) Insulin tolerance test 12 weeks after feeding with HFD or ND (55% and 12.2% calories from fat, respectively).  $n = 5$ . HFD-fed mice were compared with ND-fed mice.  $P < 0.03$  (20 minutes);  $P < 0.003$  (40 minutes);  $P < 0.005$  (60 minutes). (B) When insulin tolerance test was represented as area under the curve, the mice fed HFD were significantly insulin insensitive compared with mice fed ND.  $P < 0.13$  between groups fed ND;  $P < 0.27$  between groups fed HFD;  $P < 0.009$  between *Skp*<sup>+/−</sup> groups;  $P < 0.006$  between *Skp*<sup>−/−</sup> groups. (C) Blood glucose level after overnight fasting. Fasting blood glucose over 200 mg/dl was defined as diabetes.  $n = 5$  (*Skp2*<sup>+/−</sup> ND and *Skp2*<sup>−/−</sup> ND); 8 (*Skp2*<sup>+/−</sup> HFD); 6 (*Skp2*<sup>−/−</sup> HFD). (D) Glucose tolerance test 12 weeks after feeding with HFD. \* $P < 0.05$ ; \*\* $P < 0.01$ ; \*\*\* $P < 0.005$ .

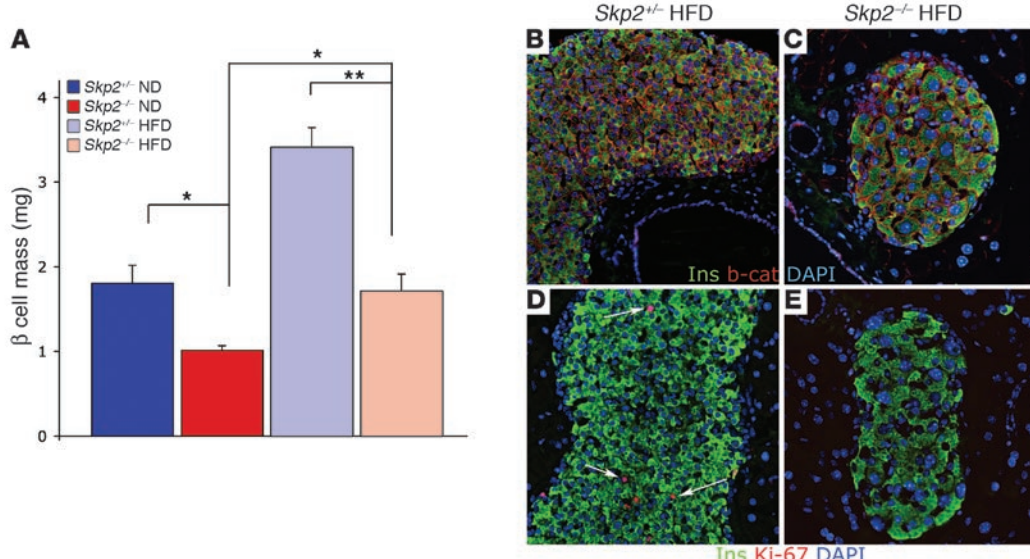
compared with *Skp2*<sup>−/−</sup> mice fed ND. The nuclear diameter of  $\beta$  cells from *Skp2*<sup>−/−</sup> mice fed HFD increased 21% in size compared with *Skp2*<sup>−/−</sup> mice fed ND (ND,  $12.75 \pm 0.39 \mu\text{m}$ ; HFD,  $15.95 \pm 0.43 \mu\text{m}$ ;  $P < 0.03$ ; Figure 7C). To assess whether increased proliferation of  $\beta$  cells was responsible for the compensatory increase in  $\beta$  cell mass in the mice fed HFD, we stained islets with Ki-67, a marker for proliferation. A number of  $\beta$  cells with nuclei that also stained for Ki-67 were readily apparent in islets from *Skp2*<sup>+/−</sup> mice fed HFD (Figure 7D). In contrast,  $\beta$  cells from *Skp2*<sup>−/−</sup> mice fed HFD that stained for Ki-67 were not observed (Figure 7E). This indicated that the increase in  $\beta$  cell mass observed in *Skp2*<sup>−/−</sup> mice fed HFD occurred in the absence of proliferation and could be attributed primarily to  $\beta$  cell hypertrophy. The combination of morphological and metabolic data suggests that adaptive changes in  $\beta$  cell mass occurs as a result of proliferation of  $\beta$  cells, and increased  $\beta$  cell size appears to be insufficient to compensate for the increased insulin resistance in the *Skp2*<sup>−/−</sup> mice fed HFD.

## Discussion

The analysis of *Skp2*<sup>−/−</sup> mice presented here reveals what we believe to be a novel role for the ubiquitin-proteasome pathway in regulating pancreatic  $\beta$  cell mass. We show here that *Skp2*-mediated p27 degradation was important not only for establishing the  $\beta$  cell mass during the postnatal growth period, but also for the adaptive expansion of the  $\beta$  cell mass in the face of increased metabolic

demand. These results directly demonstrated that  $\beta$  cell proliferation was an important ingredient in the adaptive expansion of  $\beta$  cell mass associated with insulin resistance. Moreover, it appears that the mechanisms that regulate  $\beta$  cell mass in the early postnatal period of growth were recapitulated during the adaptive expansion of  $\beta$  cell mass. These results are consistent with recent studies that demonstrated the essential role of transcription factors that link  $\beta$  cell proliferation and differentiation in the compensatory expansion of  $\beta$  cell mass associated with insulin resistance (25, 26).

Despite the fact that *Skp2* can target several proteins for proteasomal degradation, we showed that for the most part, the cellular and metabolic changes observed in *Skp2*<sup>−/−</sup> mice were rescued by simultaneous loss of p27. This indicates that p27 is a principal target of *Skp2*-dependent protein degradation in the  $\beta$  cell and consistent with prior studies in other cell types (22, 27). However, the observation that the metabolic phenotype of *p27*<sup>−/−</sup>/*Skp2*<sup>−/−</sup> mice is similar but not completely identical to that of *p27*<sup>−/−</sup> mice indicates that although p27 is a primary target of *Skp2*, *Skp2* may also mediate the ubiquitylation of other substrates that could play a role in tissues that contribute to the metabolic phenotype. In hepatocytes, like  $\beta$  cells, the absence of *Skp2* results in endoreduplication and absence of proliferation (22, 27). Recent studies show that *Skp2* also controls adipocyte proliferation and that its absence prevents adipocyte proliferation but does not affect hypertrophy (28, 29). These studies also show that the compensa-

**Figure 7**

Adaptive expansion of  $\beta$  cell mass was abrogated in  $Skp2^{-/-}$  mice. (A) Analysis of  $\beta$  cell mass 12 weeks after feeding with HFD or ND.  $n = 3$  per group. (B–E) Pancreatic sections from  $Skp2^{+/−}$  mice (B and D) and  $Skp2^{-/-}$  mice (C and E) fed HFD for 12 weeks were immunostained with antibodies to insulin (green) and to  $\beta$ -catenin (red) (B and C), or to insulin (green) and Ki-67 (red) (D and E). Arrows denote proliferating  $\beta$  cells. DAPI-stained nuclei appear blue.  $*P < 0.05$ ;  $**P < 0.01$ .

tory islet mass of  $Skp2$  mice as a result of diet-induced obesity is compromised. This reinforces that the metabolic phenotype could have complex origins and may be the result of the loss of  $Skp2$  in several interacting tissues, because all these analyses were carried out in conventional knockout mice.

Although it is known that  $\beta$  cells can respond to growth signals by either hypertrophy or proliferation, the specific determinants of  $\beta$  cell hypertrophy versus proliferation that result in expansion of  $\beta$  cell mass are poorly understood. In the  $Skp2^{-/-}$  mice, p27 accumulation inhibits mitosis and instead,  $\beta$  cells respond to growth signals by cellular hypertrophy. Thus  $Skp2$ -regulated p27 degradation is critical in determining whether  $\beta$  cells undergo proliferation or enlargement in response to growth factor signals. Moreover, the functional state of the ubiquitin-proteasome system itself could be an important indicator of whether  $\beta$  cells proliferate or undergo cellular hypertrophy. It is striking that compensatory growth by  $\beta$  cell hypertrophy in the  $Skp2^{-/-}$  mice fed HFD was insufficient to compensate for the absence of  $\beta$  cell proliferation in regulating glucose homeostasis. This observation suggests that in the absence of proliferation,  $\beta$  cells cannot maintain and regenerate islet function. This implies that the mechanism of regeneration of endocrine pancreas is quite different from the mechanism employed by other organs. For example, hepatocytes can regenerate liver mass and function solely through endoreduplication (30–32).

$Ir2^{-/-}$  and  $db/db$  mice show progressive accumulation of p27 in the nuclei of  $\beta$  cells (14). Deletion of  $p27$  allele rescued the diabetic phenotype and  $\beta$  cell mass of these mice, presumably by inducing the proliferation of  $\beta$  cells. These results are consistent with the idea that accumulation of p27 contributed to the reduction of  $\beta$  cell mass and subsequent  $\beta$  cell failure in these mice. We suggest that dysregulation of the  $Skp2$ -mediated p27 degradation is likely to contribute to the accumulation of p27 in the  $\beta$  cells of these animal models of diabetes. Dysregulation of the p27 degradation pathway could contribute to the inability of  $\beta$  cell mass to expand and to the progression of diabetes (33). It also follows that manipulating the accumulation of p27 could be a useful strategy in  $\beta$  cell regeneration.

The requirement for  $\beta$  cell proliferation in establishing  $\beta$  cell mass during postnatal and adaptive growth due to insulin resis-

tance does not rule out contributions of  $\beta$  cells derived from pancreatic stem cell sources (34). The formation of the endocrine pancreas was not affected in  $Skp2^{-/-}$  mice, indicating that  $Skp2$ -mediated p27 degradation was not required during embryogenesis in generating the proper number of  $\beta$  cells. While the findings of the present study are consistent with  $Skp2$ -mediated p27 turnover in regulating  $\beta$  cell proliferation, it is possible that p27 degradation could be required either in the self-renewal of adult pancreatic stem cells or in the transient amplifying population of  $\beta$  cell precursors. Alternatively, pancreatic stem cells could provide a pool of proliferative  $\beta$  cells that relies on  $Skp2$ -mediated p27 degradation for generating  $\beta$  cell expansion. The results presented here illustrate the importance of the ubiquitin-proteasome pathway in regulating progression of the  $\beta$  cell cycle, regulation of pancreatic  $\beta$  cell mass, and development of diabetes.

## Methods

**Animal maintenance and tissue processing.** All animal experiments were performed in accordance with NIH policies on the humane care and use of laboratory animals and approved by the Animal Research Committee of the Office for the Protection of Research Subjects at UCLA. Targeted disruption of the  $Skp2$  allele has been described previously (35). The line was maintained in heterozygotes on a C57BL/6J-CD1 mixed background. The day of birth was designated P0. DNA extracted from tails was used for PCR-based genotyping using standard methods. Primers used for genotyping were as follows: KO-specific, forward, AGAGTGGAGAACCCAGGCAGGAC; reverse, CCCGTGGAGGGAAAAAGAGGGACG; wild-type-specific, forward, GCATCGCCTTCTATCGCCTTCTTG; reverse, TTCCCACCCCCCATCCAGTCATT. Pancreatic tissue was dissected in PBS, fixed in 4% formaldehyde for 4 hours to overnight, dehydrated in grades of ethanol, and stored at  $-20^{\circ}\text{C}$  until processed for paraffin embedding.

**Immunofluorescence staining.** Pancreas sections (5  $\mu\text{m}$ ) were deparaffinized in toluene, rehydrated in grades of alcohol, and washed in  $\text{H}_2\text{O}$ . All slides were subject to antigen retrieval protocols using Antigen Unmasking Buffer (Vector Laboratories). After antigen unmasking, the slides were cooled to room temperature. All slides were permeabilized in 0.2% Triton X-100/TBS for 20 minutes, and nonspecific binding of antibodies was blocked with 0.2% Tween 20, 3% IgG-free BSA, and TBS. The following primary antibodies were used, all diluted in the blocking solution: mouse anti-Glu-



cagon (diluted 1:1,000; Sigma-Aldrich); guinea pig anti-insulin (diluted 1:500; Dako); mouse anti-p27 (diluted 1:200; Santa Cruz Biotechnology Inc.); rabbit anti-pHH3 (diluted 1:200; Upstate); anti- $\beta$ -catenin (diluted 1:200). Donkey- and goat-derived secondary antibodies conjugated to FITC or Cy3 were diluted 1:500 (Jackson ImmunoResearch Laboratories). All slides were mounted with Vectashield with or without DAPI (Vector Laboratories). Slides were viewed using a Leica DM6000 microscope, and images were acquired using Openlab software (Improvision).

**BrdU incorporation and proliferative index.** Thymidine analog BrdU (0.025 g/g body wt) was injected i.p. 2 hours before harvesting the pancreata. Pancreata were isolated and processed for histology as described above. Mouse anti-BrdU antibody (diluted 1:100; Amersham Pharmacia) and the anti-insulin antibody were diluted in the nuclease buffer provided with the BrdU antibody. The number of insulin-positive cells and insulin- and BrdU-positive cells were counted, and the proliferative index was calculated as the percentage of BrdU incorporation. At least 2,000 insulin-positive cells from the pancreatic sections spanning the whole pancreas and at least 3 mice in total were counted.

**Morphometric analysis.** The pancreata were trimmed of all nonpancreatic tissue, weighed, and processed for histology. Pancreata were embedded in paraffin such that longitudinal sections from tail to head of the pancreas were obtained. Five representative sections from each pancreas (spanning the width of the pancreas) were used in the analysis of  $\beta$  cell mass. Sections were stained with guinea pig anti-insulin antibody (diluted 1:500; Dako), followed by FITC-conjugated anti-guinea pig IgG antibody. All slides were mounted with Vectashield with DAPI (Vector Laboratories). The whole section was scanned using a Leica DM6000 microscope and montage was made using NIH ImageJ software. The cross-sectional areas of pancreata and  $\beta$  cells (insulin $^+$  cells) were determined using Openlab software. The relative cross-sectional area of  $\beta$  cells was determined by quantification of the cross-sectional area occupied by  $\beta$  cells divided by the cross-sectional area of total tissue. Each section was analyzed to estimate  $\beta$  cell and total tissue area. The  $\beta$  cell mass per pancreas was estimated as the product of the relative cross-sectional area of  $\beta$  cells per total tissue and the weight of the pancreas. The  $\beta$  cell mass was calculated by examining pancreata from at least 3 animals for each age and genotype.

**Metabolic analysis.** Glucose tolerance test was performed following overnight fast. Baseline blood glucose levels (mg/dl) were measured in saphenous vein blood from mice using OneTouch Ultra Glucose Meter (Lifescan Inc.). Glucose (2 mg dextrose/g body wt) in sterile PBS was injected i.p., and blood glucose was measured 15, 30, 60, and 120 minutes after injection. To measure plasma insulin levels, approximately 40  $\mu$ l blood was collected from the saphenous vein prior to and 30 minutes after i.p. injection with glucose (2 mg/g body wt). Blood samples were centrifuged, and serum was used to measure insulin concentrations with Insulin (mouse) Ultrasensitive EIA kit (ALPCO Diagnostics). Insulin tolerance test was performed after a 6-hour fast. Baseline blood glucose was measured before i.p. injection of insulin (0.75 mU/g body wt), and blood glucose levels were measured 20, 40, and 60 minutes after injection. Fasting blood glucose was measured following a 6-hour fast.

**Islet isolation and culture.** Liberase propidium iodide-purified enzyme-blend for rodent islet isolation (Roche Applied Science) was injected at 3.5 mg/ml into the pancreas via the bile duct after the entire abdominal cavity of the mouse was exposed. The inflated pancreas was removed and incubated in Liberase propidium iodide for 10–20 minutes at 37°C. Islets were dissociated from the exocrine tissue by manually shaking vigorously for a few minutes. The islets were separated by Histopaque (Sigma-Aldrich) gradient, followed by visual selection under a dissecting microscope. The hand-picked islets were then placed in RPMI at 37°C under a 95% air, 5% CO<sub>2</sub> mixture for approximately 24 hours before being used for the experiments.

Islets were either lysed or used directly after isolation for RT-PCR, Western blot, or FACS analysis.

**Measurement of insulin secretion by islet perfusion.** The insulin secretion characteristics of islets were studied in an islet perfusion system (ACUSYST-S; Cellex Biosciences) as previously described (36). In brief, after overnight culture, 10–15 islets were suspended in Bio-Gel P-2 beads (Bio-Rad) and placed into the 500- $\mu$ l perfusion chambers. Islets were equilibrated in Kreb's Ringer bicarbonate buffer (115 mM NaCl, 4.7 mM KCl, 2.5 mM CaCl<sub>2</sub>, 1.2 mM KH<sub>2</sub>PO<sub>4</sub>, 1.2 mM MgSO<sub>4</sub>·7H<sub>2</sub>O), 20 mM HEPES (pH 7.4), 0.2% BSA (Sigma-Aldrich), and 4 mM glucose at 37°C. At the beginning of the experiment, samples were collected from islets exposed to a basal glucose concentration of 4 mM before increasing glucose concentration from 4 to 16 mM. A flow rate of 0.35 ml/min was used, with each fraction containing 0.35 or 1.4 ml of effluent. After stimulating with 16 mM glucose for 40 minutes, the islets were again equilibrated in Kreb's buffer with 4 mM glucose for 20 minutes before being exposed to 20 mM KCl to detect the insulin secretion ability independent of glucose stimulation. For insulin content measurements, cells were lysed in islet lysis buffer containing 100 mM HEPES and 0.8% Triton X-100 under mild sonication. The insulin levels in secretion buffer and extracts were quantified by Insulin (mouse) Ultrasensitive EIA kit (ALPCO Diagnostics).

**Flow cytometric analysis of DNA content.** Single islet cells for determination of DNA content were prepared by digesting the isolated islets with 1 mM trypsin solution for 10–15 minutes at 37°C. The cells obtained were permeabilized with -20°C 70% ethanol dropwise while vortexing, and kept at -20°C. On the day of DNA staining, the ethanol was removed by spinning down the cells at 250 g for 5 minutes. The cells were then stained with 0.01% propidium iodide (Calbiochem) solution for 15–30 minutes. All analyses were performed with a FACSCan flow cytometer and CellQuest software (BD).

**HFD treatment.** From the age of 5 weeks, mice were fed with either a HFD containing 55% calories from fat (TD 93075; Harlan Teklad) or ND containing 12.2% calories from fat (TD 8604; Harlan Teklad) for a period of 13 weeks. Body weights and food intake were recorded every week, and fasting blood glucose level (6 hours) was measured every 2 weeks. The mice with fasting blood glucose levels greater than 200 mg/dl were considered diabetic. Glucose and insulin tolerance test assays were performed 12 weeks after beginning the diet.

**Statistics.** All data were expressed as mean  $\pm$  SEM. The statistical significance of differences was measured by unpaired 2-tailed Student's *t* test. A *P* value of less than 0.05 indicated statistical significance.

## Acknowledgments

We acknowledge receiving technical help in histology from Rosemary Soliz and Aleksey Matveyenko in islet perfusion studies. We are grateful to James Roberts for *p27*<sup>-/-</sup> mice and Peter Butler for helpful discussions. Flow cytometry was performed in the UCLA Jonsson Comprehensive Cancer Center (JCCC) and Center for AIDS Research Flow Cytometry Core Facility. S. Georgia is supported by the Ruth L. Kirschstein National Research Service Award GM07185. This work was supported by grants from the NIH (R01 DK-068763) and the Larry Hillblom and Juvenile Diabetes Research Foundation to A. Bhushan.

Received for publication March 22, 2007, and accepted in revised form June 12, 2007.

Address correspondence to: Anil Bhushan, Larry Hillblom Islet Research Center, David Geffen School of Medicine, UCLA, 900A Weyburn Place, Los Angeles, California 90095, USA. Phone: (310) 206-5750; Fax: (310) 206-5368; E-mail: ABhushan@mednet.ucla.edu.



1. Bruning, J.C., et al. 1997. Development of a novel polygenic model of NIDDM in mice heterozygous for IR and IRS-1 null alleles. *Cell*. **88**:561–572.
2. Accili, D. 2001. A kinase in the life of the  $\beta$  cell. *J. Clin. Invest.* **108**:1575–1576.
3. Bonner-Weir, S. 2000. Islet growth and development in the adult. *J. Mol. Endocrinol.* **24**:297–302.
4. Lingohr, M.K., Buettner, R., and Rhodes, C.J. 2002. Pancreatic beta-cell growth and survival – a role in obesity-linked type 2 diabetes? *Trends Mol. Med.* **8**:375–384.
5. Butler, A.E., et al. 2003. Beta-cell deficit and increased beta-cell apoptosis in humans with type 2 diabetes. *Diabetes*. **52**:102–110.
6. Flier, S.N., Kulkarni, R.N., and Kahn, C.R. 2001. Evidence for a circulating islet cell growth factor in insulin-resistant states. *Proc. Natl. Acad. Sci. U. S. A.* **98**:7475–7480.
7. Bonner-Weir, S. 2000. Perspective: Postnatal pancreatic beta cell growth. *Endocrinology*. **141**:1926–1929.
8. Heit, J.J., Karnik, S.K., and Kim, S.K. 2006. Intrinsic regulators of pancreatic beta-cell proliferation. *Annu. Rev. Cell Dev. Biol.* **22**:311–338.
9. Cozar-Castellano, I., et al. 2006. Molecular control of cell cycle progression in the pancreatic beta-cell. *Endocr. Rev.* **27**:356–370.
10. Kushner, J.A. 2006. Beta-cell growth: an unusual paradigm of organogenesis that is cyclin D2/Cdk4 dependent. *Cell Cycle*. **5**:234–237.
11. Georgia, S., and Bhushan, A. 2006. Cell cycle regulation and beta cells. In *Islet cell growth factors*. R. Kulkarni, editor. Landes Bioscience. Austin, Texas, USA.
12. Rane, S.G., et al. 1999. Loss of Cdk4 expression causes insulin-deficient diabetes and Cdk4 activation results in beta-islet cell hyperplasia. *Nat. Genet.* **22**:44–52.
13. Georgia, S., and Bhushan, A. 2006. p27 regulates the transition of beta-cells from quiescence to proliferation. *Diabetes*. **55**:2950–2956.
14. Uchida, T., et al. 2005. Deletion of Cdkn1b ameliorates hyperglycemia by maintaining compensatory hyperinsulinemia in diabetic mice. *Nat. Med.* **11**:175–182.
15. Lin, D.I., and Diehl, J.A. 2004. Mechanism of cell-cycle control: ligating the ligase. *Trends Biochem. Sci.* **29**:453–455.
16. Vlach, J., Hennecke, S., and Amati, B. 1997. Phosphorylation-dependent degradation of the cyclin-dependent kinase inhibitor p27. *EMBO J.* **16**:5334–5344.
17. Montagnoli, A., et al. 1999. Ubiquitination of p27 is regulated by Cdk-dependent phosphorylation and trimeric complex formation. *Genes Dev.* **13**:1181–1189.
18. Sheaff, R.J., Groudine, M., Gordon, M., Roberts, J.M., and Clurman, B.E. 1997. Cyclin E-CDK2 is a regulator of p27Kip1. *Genes Dev.* **11**:1464–1478.
19. Carrano, A.C., Eytan, E., Hershko, A., and Pagano, M. 1999. SKP2 is required for ubiquitin-mediated degradation of the CDK inhibitor p27. *Nat. Cell Biol.* **1**:193–199.
20. Sutterluty, H., et al. 1999. p45SKP2 promotes p27Kip1 degradation and induces S phase in quiescent cells. *Nat. Cell Biol.* **1**:207–214.
21. Tsvetkov, L.M., Yeh, K.H., Lee, S.J., Sun, H., and Zhang, H. 1999. p27(Kip1) ubiquitination and degradation is regulated by the SCF(Skp2) complex through phosphorylated Thr187 in p27. *Curr. Biol.* **9**:661–664.
22. Nakayama, K., et al. 2004. Skp2-mediated degradation of p27 regulates progression into mitosis. *Dev. Cell.* **6**:661–672.
23. Nakayama, K., et al. 2000. Targeted disruption of Skp2 results in accumulation of cyclin E and p27(Kip1), polyploidy and centrosome overduplication. *EMBO J.* **19**:2069–2081.
24. Georgia, S., and Bhushan, A. 2004.  $\beta$  cell replication is the primary mechanism for maintaining postnatal  $\beta$  cell mass. *J. Clin. Invest.* **114**:963–968. doi:10.1172/JCI200422098.
25. Okamoto, H., et al. 2006. Role of the forkhead protein FoxO1 in  $\beta$  cell compensation to insulin resistance. *J. Clin. Invest.* **116**:775–782. doi:10.1172/JCI24967.
26. Kulkarni, R.N., et al. 2004. PDX-1 haploinsufficiency limits the compensatory islet hyperplasia that occurs in response to insulin resistance. *J. Clin. Invest.* **114**:828–836. doi:10.1172/JCI200421845.
27. Kossatz, U., et al. 2004. Skp2-dependent degradation of p27kip1 is essential for cell cycle progression. *Genes Dev.* **18**:2602–2607.
28. Auld, C.A., Fernandes, K.M., and Morrison, R.F. 2007. Skp2-mediated p27(Kip1) degradation during S/G2 phase progression of adipocyte hyperplasia. *J. Cell Physiol.* **211**:101–111.
29. Sakai, T., et al. 2007. Skp2 controls adipocyte proliferation during the development of obesity. *J. Biol. Chem.* **282**:2038–2046.
30. Lazzarini Denchi, E., Celli, G., and de Lange, T. 2006. Hepatocytes with extensive telomere deprotection and fusion remain viable and regenerate liver mass through endoreduplication. *Genes Dev.* **20**:2648–2653.
31. Minamishima, Y.A., Nakayama, K., and Nakayama, K. 2002. Recovery of liver mass without proliferation of hepatocytes after partial hepatectomy in Skp2-deficient mice. *Cancer Res.* **62**:995–999.
32. Wirth, K.G., et al. 2006. Separase: a universal trigger for sister chromatid disjunction but not chromosome cycle progression. *J. Cell Biol.* **172**:847–860.
33. White, M.F. 2003. Insulin signaling in health and disease. *Science*. **302**:1710–1711.
34. Dor, Y., Brown, J., Martinez, O.I., and Melton, D.A. 2004. Adult pancreatic beta-cells are formed by self-duplication rather than stem-cell differentiation. *Nature*. **429**:41–46.
35. Nakayama, K., et al. 1996. Mice lacking p27(Kip1) display increased body size, multiple organ hyperplasia, retinal dysplasia, and pituitary tumors. *Cell*. **85**:707–720.
36. Song, S.H., Rhodes, C.J., Veldhuis, J.D., and Butler, P.C. 2003. Diazoxide attenuates glucose-induced defects in first-phase insulin release and pulsatile insulin secretion in human islets. *Endocrinology*. **144**:3399–3405.